J. Sci. I. R. Iran

Vol.9 No.3
Summer 1998

LIQUEFACTION POTENTIAL ASSESSMENT USING MULTILAYER ARTIFICIAL NEURAL NETWORK

S.M. Fatemi Aghda,[1] M. Teshnehlab,[2] A. Suzuki, T. Akiyoshi and Y. Kitazono[3]

[1]*Department of Geology, Tarbiat Moallem University, Tehran, Islamic Republic of Iran*
[2]*K.N.T. University of Technology, Faculty of Electrical Engineering, Tehran, Islamic Republic of Iran*
[3]*Department of Civil and Environmental Engineering, Kumamoto University, Kumamoto, Japan*

Abstract

In this study, a low-cost, rapid and qualitative evaluation procedure is presented using dynamic pattern recognition analysis to assess liquefaction potential which is useful in the planning, zoning, general hazard assessment, and delineation of areas. Dynamic pattern recognition using neural networks is generally considered to be an effective tool for assessing of hazard potential on the basis of established criteria. In this paper, the classification operation, in which an input pattern is passed to the network and the network produces a representative class as output, is considered for evaluation of liquefaction hazard potential. The application of Multilayer Artificial Neural Network for the prediction of liquefaction was examined in the northwest of Iran (Gilan Plain). The study area suffered a catastrophic earthquake in June 1990 and most of the damage to lifeline facilities and structures in urban areas was brought about by liquefaction phenomena. The simulated results by multilayer artificial neural network in this study revealed the high capability of this method to predict the liquefaction potential of soils.

Introduction

A major cause of earthquake damage in soft ground is liquefaction. During the 1964 Niigata earthquake [1], 1964 Alaska earthquake [2], 1977 Varancea earthquake [3], 1983 Nihonkai-chubu earthquake [4], 1989 Loma prieta earthquake [5], 1990 Iran-Manjil earthquake [6] etc., with various magnitude, major damage was caused by liquefaction phenomenon. The geotechnical aspects of liquefaction during the past earthquakes were mostly: large and differential settlement, tilting and collapse of structures, sand volcanoes and sand boiling, floating up of wooden piles and light weight foundation structures, landslides, and damage to buried pipelines, roads, plowed fields, dikes of rivers, and other lifeline facilities.

Various procedures have been developed for liquefaction potential assessment of saturated soils such as methods using SPT N-value and/or relative density and mean particle size of soil grains [4,7,8,9]. Based on

Keywords: Hazard rate; Liquefaction potential; Multilayer artificial neural network; Prediction

these procedures, several techniques have been proposed for the microzonation of liquefaction hazard, such as the technique of compiling two constituent maps (ground failure susceptibility map and ground failure opportunity map) as presented by Youd [10] and Elton [11]; liquefaction severity index mapping, Youd [12]; and probabilistic liquefaction potential mapping as presented by Kavazanjian [13], which are compilations of both ground failure susceptibility and ground failure opportunity maps, or only one of those.

The proposed method in this paper can simultaneously consider both opportunity and the ground's susceptibility to liquefaction, on the available information, and simulate the ground's liquefaction potential, a method useful for regional and areal scale applications.

Liquefaction Evaluation Criteria

Factors Influencing the Liquefaction Potential of Soils

Based on a comprehensive review of the literature on the subject, past observations, and a field study in the northwestern part of Iran where more than ten slope failures and liquefaction phenomena occurred as a result of the 1990 Iran-Manjil earthquake, heavy rainfall and human activities, the most important factors in liquefaction phenomena are the geological, geomorphological, seismic and geotechnical characteristics of the ground. Evaluation criteria for liquefaction hazard will be presented here. Because the criteria were established on the basic characteristics of the hazards, and the most significant properties of past observations in the world were considered in their selection, they will, no doubt, find global application.

As the liquefaction potential of any soil deposit is affected by the soil properties, environmental factors, and characteristics of the earthquake [8], among the many factors which may have some influence on the liquefaction potential of soils, the following eight items are selected from a comprehensive review of the literature on the subject, past experience, and engineering judgment, etc..

1. Geological characteristics of site
2. Geomorphological characteristics of site
3. Relative site amplification
4. Intensity increments
5. Sandy layer thickness
6. Water table level
7. Surface layer thickness
8. Type of soil

Each item has five to 29 factors. A total of eight factors were adopted for evaluation of liquefaction potential in each mesh or point by using geological and topographical maps, seismic characteristics by considering the geological aspects of the area, and geotechnical features of the area.

The considered criteria are defined for those earthquakes which had a minimum magnitude of 5.2 and which induced liquefaction in the world, on the basis of a comprehensive review of published papers on reported earthquakes in various countries.

Geological and Geomorphological Criteria

Geological and geomorphological factors directly or indirectly influence geotechnical properties that control the liquefaction susceptibility of sediments. Thus, the correlation between past liquefaction occurrence with geological and geomorphological parameters is the best way of clarifying the reliability of these factors in the prediction of liquefaction.

The geological criteria were established on the susceptibility of geological units to liquefaction given by Youd [10]. According to the geological criteria, the susceptibility of sediments to liquefaction is determined by considering their age. In this criterion, the recent deposits are those which are less than 500 years old. The selected geological criteria are given in Table 1.

Table 2 shows the liquefaction susceptibility chart of geomorphological setting for characterizing the liquefaction potential, given by Wakamatsu [14]. These criteria, which have been made based on the site specific correlation between past liquefaction occurrences and geologic and geomorphological settings, can be used to identify the liquefaction potential of sediments.

Seismicity Criteria

The characteristics of earthquake ground motions are affected by several factors such as source, path and site effects, but it has been pointed out that variation of site effects is very large. Although the attenuation relations give the ground motion intensity on reference ground, observations during past earthquakes have suggested that variations in the intensity of shaking are significantly dependent on local site conditions. For evaluation of liquefaction opportunity, the main factors are sources and attenuation of earthquakes.

But recognition of source distribution and attenuation characteristics of earthquakes, especially in areas covered by thick sediments, is difficult. Thus, the seismic intensity increments and relative site amplifications can be considered as appropriate surrogate measures suitable for liquefaction hazard evaluation.

The empirical correlations between the surface geology and seismic intensity increments have been established by many investigators, among them

Medvedev [15], Evernden [16], Kagami [17], and Astroza [18], are based on observations during earthquakes in Central Asia, California, Japan, and Chile, respectively. The Medvedev criteria are used in this study and are shown in Table 3.

Another seismic criterion is presented in terms of relative site amplifications which were proposed by Borcherdt [19] to evaluate the effects of site geology by measuring generated ground motions during nuclear explosions at sites with various geological conditions and by calculating the spectral amplifications of the motions with respect to those at granite rock. They found a strong correlation between surface geology and the average horizontal spectral amplification which is the average of the spectral amplification in the frequency range of 0.5 to 2.5 Hz.

The selected criteria give the values of the relative amplifications for different soils, which were proposed by Shima [20], based on the analytical calculation of seismic response of ground. This is the ratio of the maximum value of ground response in the frequency range of 0.1 to 10 Hz, with respect to that at loam ground. These criteria are illustrated in Table 4.

Geotechnical Criteria

The geotechnical criteria consist of thickness of

Table 1. Susceptibility of geological items to liquefaction (after Youd and Perkins, 1987)

Geological category (Type of deposits)	Susceptibility of sediments considering their age			
	Recent	Holocene	Pleistocene	Pre-Pleistocene
River channel	A	B	D	E
Delta	A	B	D	E
Uncompacted fill	A	-	-	-
Flood plain	B	C	D	E
Delta and fan delta	B	C	D	E
Lacustrine and playa	B	C	D	E
Colluvium	B	C	D	E
Dunes	B	C	D	E
Loess	B	B	B	E
Tephra	B	B	E	E
Sebka	B	C	D	E
Estuarine	B	C	D	E
Beach low wave energy	B	C	D	E
Lagoonal	B	C	D	E
Foreshore	B	C	D	E
Alluvial fan and plain	C	D	D	E
Marine terraces and plains	C	D	E	E
Beach high wave energy	C	D	E	E
Talus	D	D	E	E
Glacial till	D	D	D	E
Tuff	D	D	D	E
Residual soils	D	D	E	E
Compacted fill	D	-	-	-
Others	E	E	E	E

A = Very high liquefaction susceptibility; B = High liquefaction susceptibility; C = Moderate liquefaction susceptibility; D = Low liquefaction susceptibility; E = Very low liquefaction susceptibility

sandy layers, water table, surface layer's thickness, and type of soils. These criteria are given in Table 5 and were established based on past observations of liquefied and nonliquefied sites during earthquakes.

The likelihood of the occurrence of liquefaction in sandy layers with a thickness of more than 3 m is assumed to be very high, while in those with a thickness of less than 0.5 m the susceptibility to liquefaction is very low. For water table depths greater than 10 m, the likelihood of liquefaction in most deposits is very low, while for those of less than 1 m this likelihood is very high. Also, the susceptibility of layers of more than 10 m in depth to liquefaction is very low, while that of layers of less than 3 m depth is very high. Since liquefaction is the most common phenomena during earthquakes in loose sandy soils, the type and grain size of sandy soils were considered as effective factors in liquefaction occurrence. Consequently, the distance between very

Table 2. Susceptibility of geomorphological items to liquefaction (after Japan Working Group, 1992).

Geomorphological units	Susceptibility of units to liquefaction
Natural levee (edge)	A
Abandoned river channel	A
Former pond	A
Dry river bed consisting of sandy soils	A
Sand dune (lower slope of sand dune)	A
Artificial beach	A
Interlevee low land	A
Reclaimed land by drainage	A
Reclaimed land or filled land	A
Spring	A
Fill on boundary zone between sand dune and low land	A
Fill adjoining cliff	A
Fill on marsh swamp	A
Fill on reclaimed land by drainage	A
Other type of fill	A
Alluvial fan with vertical gradient more than 0.5%	B
Valley plain consisting of sandy soils	B
Natural levee (top)	B
Back marsh	B
Marsh and swamp	B
Delta	B
Sand bar	B
Beach	C
Valley plain consisting of gravel or cobble	D
Alluvial fan with vertical gradient more than 0.5%	D
Dry river bed consisting of gravel	D
Gravel bar	D
Sand dune (top of sand dune)	D
Others	E

A = Very high liquefaction susceptibility; B = High liquefaction susceptibility; C = Moderate liquefaction susceptibility; D = Low liquefaction susceptibility; E = Very low liquefaction susceptibility

Table 3. Intensity increments of ground (Medvedev, 1962)

Geological units	Rating
Granites	E
Limestone, sandstone and shales	D
Gypsum and marl	D
Coarse material ground	C
Sandy ground	C
Clayey ground	C
Fill	B
Moist ground	B
Moist fill and soil ground	A

A = Very high; B = High; C = Moderate; D = Low; E = Very low

Table 4. Relative site amplification of ground (after Shima, 1978).

Geological units	Rating
Peat	A
Humus	B
Clay	B
Loam	C
Sand	D
Others	E

A = Very high; B = High; C = Moderate; D = Low; E = Very low

high to very low likelihood to liquefaction of soil layers is divided into five intervals that are given by alphabetical symbols from A to E.

The Structure of Artificial Neural Networks

Neural networks are information processing systems. In general, neural networks can be thought of as black boxes, devices that accept inputs and produce outputs. In order to process information, the neural networks perform several operations: classification; pattern recognition; pattern completion; noise removal; optimization; and control [21-23].

layers: an input layer, Fx, which consists of the PEs $x_1,x_2,x_3,\ldots,x_n$; a hidden layer, Fy, which consists of the PEs, $y_1,y_2,y_3,\ldots y_n$; and an output layer, Fz, which consists of the PEs $z_1,z_2,z_3,\ldots z_n$. The PEs are connected with weighted connections. In Figure 1 there are weighted connections from every Fx to every Fy (from input to hidden layers), and there are weighted connections from every Fy to every Fz (from hidden to output layers). The connection weights store the information in the form of weights matrices (Fig. 1). The value of the connection weights is determined by the neural network learning procedure. Then the PEs are the portion of neural networks

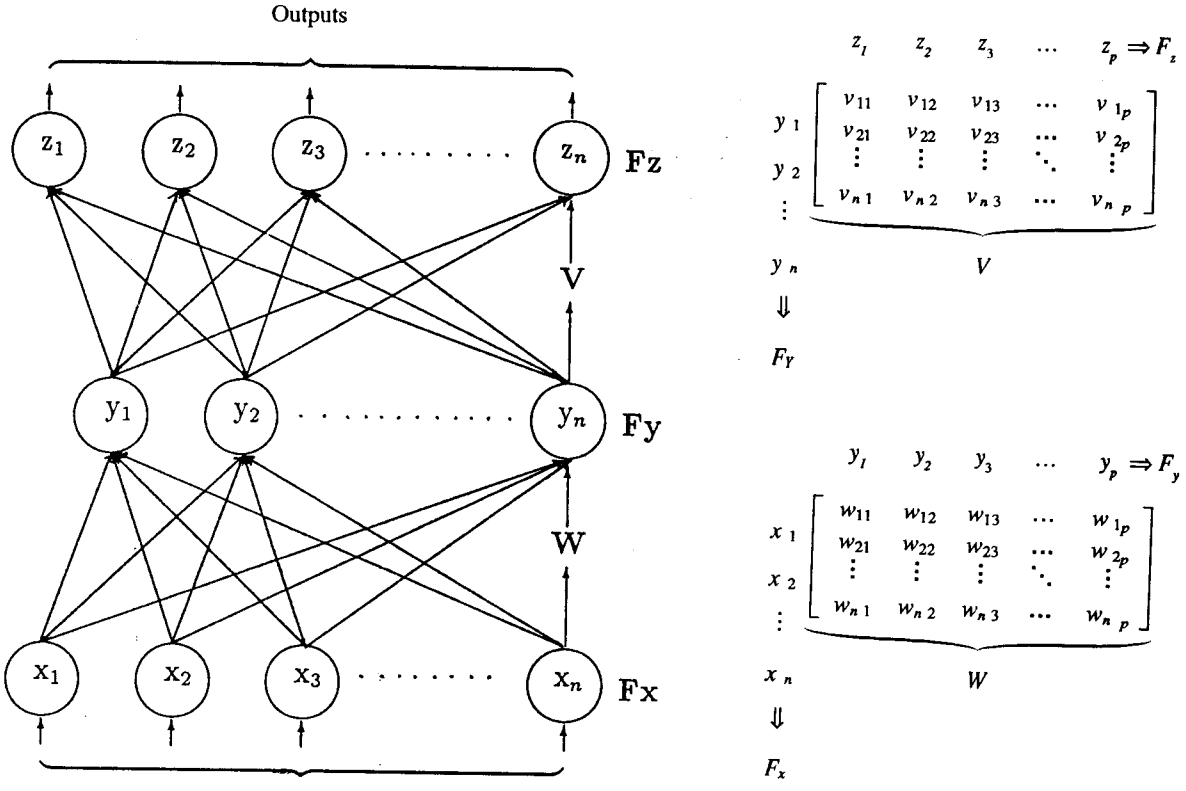

Figure 1. The topology of a three layer neural network [21]

The basic elements of neural networks are processing elements (PEs) and weighted concentrations. The collection of processing elements in neural networks, as a layer, includes an input layer; one or more hidden layers; and an output layer. Each processing element in a neural network collects the values from all of its input connections, performs a predefined mathematical operation and produces a single output value [24-25]. Figure 1 depicts a typical neural network with three

that perform all the computing of outputs.

Among the several types of neural networks, multilayer neural networks are used for pattern classification, pattern matching and function approximation. Using continuously differentiable PE functions, such as Gaussian or sigmoid functions in a multilayer neural network, the network can learn practically any nonlinear mapping to any desired degree of accuracy.

Learning is the most appealing quality of neural networks, and determines the values of connection weights. It is defined as a change in connection weight values that results in the capture of information that can be later recalled.

Among several learning procedures, the error correction learning has the ability to adjust connection weights to learn nonlinear mapping in multilayer neural networks.

Error correction learning adjusts the connection weights between PEs in proportion to the difference between the desired and computed values of each output layer PE. The multilayer error correction learning is able to capture nonlinear mappings between the inputs and outputs. The most popular technique for learning in multilayer neural networks is the back-propagation learning method (BPM). The BPM is a systematic method for training the multilayer neural network and is one of the computationally efficient methods for the adjustment of the weights of a neural network. In such a method, the partial derivatives of an error criterion with respect to the weights are in turn adjusted along the negative gradient to minimize the error function. The structure of the weights matrices, used to compute the derivatives, is seen to be identical to that in the original network, while the input data flow in the opposite direction, justifying the term of back-propagation which is depicted in Figure 2.

The stored information must then be retrieved through a learning procedure for recognition of new input data. The process of retrieving stored information is called a recall technique.

Type of Neural Network Used in This Study

The neural network system employed in this study has three layers which are input, hidden, and output

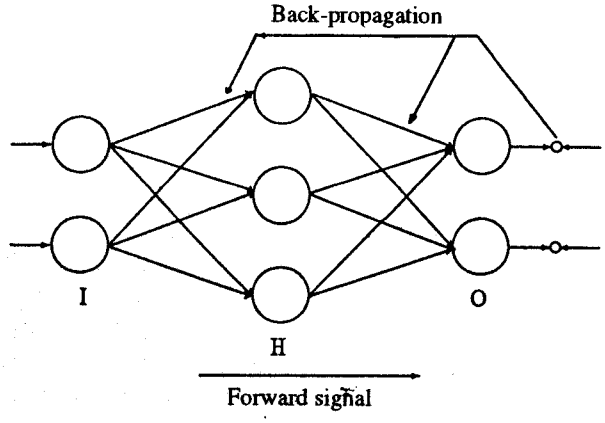

Figure 2. The structure of back-propagation learning method (BPM) [21]

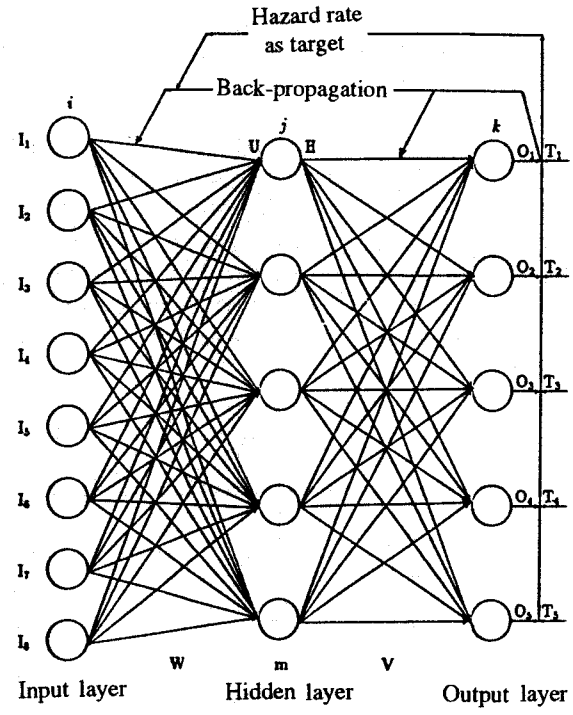

Figure 3. Error correction learning (back-propagation method) using sigmoid function units

layers. A system network, such as the typical three layer neural network given in Figure 3, is used successfully in pattern recognition. F(.) denotes sigmoid function, I is input pattern, H and O are output of hidden and output layers, respectively. The elements of W and V are adjustable weights, where the weights are adjusted to minimize the error function.

The pattern classification system consists of five completely distinct classes in which each class is represented by eight different effective items and each item has five categories that are numbered from 1 to 5 signifying very high, high, moderate, low, and very low. These terms express the liquefaction potential of soils on the basis of geological and geomorphological characteristics of the site, relative site amplification and intensity increments of the ground during an earthquake, and rating scale of geotechnical items for occurrence of liquefaction given in Tables 1 to 5.

The input window consists of a 16*16 data matrix (256 neurons) according to the number of data, in which the inputs are considered as to the pixels in the binary 0 and 1; the hidden layer has five neurons and the output layer has five patterns in order to classify five different classes as a hazard potential. Thus, according to the numbers of classes, there are five input classes and five simulating outputs (desired values of output patterns) corresponding to the five individual classes.

The input patterns, (I), are selected on the basis of eight criteria given in Tables 1 to 5. They are identified in the forms of 1, 11, 111, 1111, and 11111 for symbols of A, B, C, D, E, and their delimiter is 0. For example the input pattern of (A, B, B, C, D, E, A, C) will be shown as a pattern of (10110110111011111011111010111). The patterns for simulation are illustrated in Table 6. The simulating outputs are considered as an actual liquefaction potential of the soils and the desired values (targets) as being between 0.2 to 1.0, as a rate of liquefaction potential hazard. In this case, output around 1.0 represents very high liquefaction potential; around 0.8 high liquefaction potential; around 0.6 moderate liquefaction potential; around 0.4 low liquefaction potential; and around 0.2 shows a very low liquefaction potential (Table 7). The result of simulation with 350 learning and 100 iteration, which is shown in Table 8, reveals that the difference between actual outputs and desired outputs is very low for class Nos. 1 and 2, and is 0 for other classes. The simulation results suggest that the neural network system

Table 5. Susceptibility of geotechnical items to liquefaction

Thickness of sandy layers (T)	Rating	Water table (W.T)	Rating
T>3m	A	W.T<1m	A
2m<T≤3m	B	1m≤W.T<3m	B
1m<T≤2m	C	3m≤W.T<5m	C
0.5m<T≤1m	D	5m≤W.T<10m	D
T<0.5m	E	W.T≤10m	E
Thickness of surface layers (T.S)	**Rating**	**Type of soil**	**Rating**
T.S<3m	A	SP	A
3m≤T.S<5m	B	SW	B
5m≤T.S<7m	C	SM	C
7m≤T.S<9m	D	SC	D
T.S≥9m	E	Others	E

A = Very high liquefaction susceptibility; B = High liquefaction susceptibility; C = Moderate liquefaction susceptibility; D = Low liquefaction susceptibility; E = Very low liquefaction susceptibility

Table 6. Input patterns on the basis of eight considered criterion

Pattern No.	Input Patterns
1	101011110101010101
2	1101101111011011011011
3	11101110111011101110111011101110111
4	1111011110111101111011110111101111011101111
5	11111011111011111011111011111011111011111011111

Pattern No. 1: Very high liquefaction potential rate; the pattern is (A,A,D,A,A,A,A,A)
Pattern No. 2: High liquefaction potential rate; the pattern is (B,B,D,B,B,B,B,B)
Pattern No. 3: Moderate liquefaction potential rate; the pattern is (C,C,C,C,C,C,C,C)
Pattern No. 4: Low liquefaction potential rate; the pattern is (D,D,D,D,D,D,D,D)
Pattern No. 5: Very low liquefaction potential rate; the pattern is (E,E,E,E,E,E,E,E)

Table 7. The desired values (targets)

Pattern No.	O_1	O_2	O_3	O_4	O_5
1	**1.00**	0.00	0.00	0.00	0.00
2	0.00	**0.80**	0.00	0.00	0.00
3	0.00	0.00	**0.60**	0.00	0.00
4	0.00	0.00	0.00	**0.40**	0.00
5	0.00	0.00	0.00	0.00	**0.20**

O_1= Output of class No. 1; O_2= Output of class No. 2; O_3= Output of class No. 3; O_4= Output of class No. 4; O_5= Output of class No. 5

can be used for the fast prediction and microzonation of liquefaction potential of soils or potential slope failure. An example of pattern recognition results using the proposed method is shown in Table 9. The biggest number in each class shows that the rating value of hazard potential corresponds to its output patterns class.

The test of different classes with different patterns reveals the high ability and flexibility of multilayer neural networks for the prediction of natural hazards on a regional or areal scale.

The System Equations and Learning Back-Propagation Training Algorithm

The system equations of the artificial neural networks with five units according to Figure 3 is considered as follows; the input and output of the unit j in the hidden layer denoted by U_j and H_j, respectively, are described:

$$U_j = \sum_{i=1}^{n} W_{ji} I_i + \theta_j \quad (1)$$

$$H_j = F(U_j) = \frac{1}{1 + \exp(-2U_j / \mu_0)} \quad (2)$$

where n is the number of neurons in input layer, I_i, θ_j, and μ_0 are input neurons, a threshold in the hidden layer and the sigmoid parameter, respectively. The activation function, $F(.)$, is commonly chosen to be the sigmoid in order to resemble the state output of biological neurons which originally inspires the networks. The outputs of the hidden layer units are then transmitted to the inputs of the output layer units through another network weight

Table 8. The simulation results of different patterns

Pattern No.	O_1	O_2	O_3	O_4	O_5
1	**0.9954**	0.0008	0.0020	0.0018	0.0030
2	0.0022	**0.7999**	0.0033	0.0040	0.0000
3	0.0028	0.0034	**0.6000**	0.0001	0.0043
4	0.0037	0.0038	0.0002	**0.4000**	0.0044
5	0.0011	0.0000	0.0038	0.0040	**0.2000**

O_1= Output of class No. 1; O_2= Output of class No. 2; O_3= Output of class No. 3; O_4= Output of class No. 4; O_5= Output of class No. 5

Table 9. The examined pattern recognition results

Pattern No.	O_1	O_2	O_3	O_4	O_5
1	**0.9953**	0.0015	0.0442	0.0008	0.0019
2	0.0117	**0.4727**	0.0087	0.0024	0.0001
3	0.0151	0.0010	**0.4910**	0.0003	0.0035
4	0.0181	0.0054	0.0004	**0.1864**	0.0010
5	0.0011	0.0001	0.0032	0.0057	**0.1425**

O_1= Output of class No. 1; O_2= Output of class No. 2; O_3= Output of class No. 3; O_4= Output of class No. 4; O_5= Output of class No. 5

denoted by V_{kj}. Then the input and ouput of output layer is expressed respectively as follows.

$$S_k = \sum_{j=1}^{m} V_{kj} H_j + \gamma_k , \quad (3)$$

$$O_k = F(S_k) \quad (4)$$

Where m is the number of neurons in hidden layers, H_j is output of hidden layers and γ_k is threshold in output layer.

The weights W_{ji} and V_{kj} can be adjusted to minimize error back-propagation for the set of training patterns by a straightforward application of gradient descent. Eventually, the algorithm of BPM for our three layer neural network is expressed as follows;

$$V_{kj} = V_{kj} + \alpha\delta_k H_j, \quad (5)$$

$$W_{ji} = W_{ji} + \alpha\sigma_j I_i, \quad (6)$$

$$\gamma_k = \gamma_k + \beta\delta_k, \quad (7)$$

$$\theta_j = \theta_j + \beta\sigma_j, \quad (8)$$

where

$$\delta_k = (T_k - O_k)\, O_k(1 - O_k), \quad (9)$$

$$\sigma_j = \sum_{k=1}^{m} \delta_k V_{kj} H_j \ (1 - H_j) \quad (10)$$

and α and β are learning rate coefficients; δ and σ are the difference between the desired or target output (T) and the actual output (O); i, j and k are the neurons of input, hidden and output layers (Fig. 3).

Further advantages of neural networks have been presented in the literature [27-30]. This kind of neural network is flexible in structure design and learning capabilities.

The Examine of Recognition

The ability of the multilayer neural network to predict the liquefaction potential of soils was examined by assessing the liquefaction potential of Gilan plain in the northwest of Iran in a case study. The study area suffered a devasting earthquake ($Ms = 7.7, M_b = 6.4, M_w = 7.3$) [31] on 20 June 1990 (1990 Iran-Manjil earthquake). The widespread liquefaction in urban areas and on farmlands, mostly along the channel of the Sefied Roud river, several huge landslides, rockfalls and rockslips were the geotechnical aspects of the earthquake [6].

Based on the lithological characteristics of the area, the subsoil of the area consists of a thick sequence of low consolidated sediments sensitive to compaction. The ground water in the plain area is close to the surface. There are several rivers in the area which flow into the Caspian sea, one of the most significant of them being the Sefied Roud river. Previous observations by the first author have shown that the levee deposits are susceptible to liquefaction more than other sediments on the plain [32-33]. The geological features of the studied area and the location of boreholes are given in Figure 4.

Data Analysis

Based on the selected and established criteria (Tables 1-5) consisting of geological; geomorphological; relative site amplification and intensity increments; and geotechnical criteria including sandy layer thickness, water table depth, and surface layer thickness, the items were determined on each mesh by using data from geological and geomorphological maps, existing boreholes log, grain size distribution curves of soils [34-35], and seismic behaviour of soils. Using desired criteria for input patterns given in Table 7 and determined items for each mesh, the input patterns for each mesh were determined. The obtained input patterns were put into the multilayer neural network as new input data and were classified into corresponding classes by using pattern recognition of neural network system and liquefaction potential of each mesh recognized. Table 9 shows an example of pattern recognition obtained by the system, in which each class shows the simulated liquefaction potential of each corresponding output.

The calculated liquefaction potential of all meshes for the area is given in Table 10. The comparison of simulation results of liquefaction potential using multilayer neural network in the Gilan area and obtained results by geotechnical data base system of the area [34] revealed the high accuracy and high capability of the proposed system for the prediction of the liquefaction potential of soils.

Discussion and Conclusion

In this contribution, we developed a new method for the prediction of natural hazards such as liquefaction or slope failure phenomena. Our proposed method demonstrated a high ability with high accuracy to predict natural hazards, this ability being related to multilayer neural networks. This study provides a new focus for an experimental approach as compared with other methods [10, 11, 12, 13]. In other methods, the liquefaction potential is expressed by the compilation of liquefaction susceptibility and liquefaction opportunity maps, the susceptibility of soils to liquefaction and the capability of earthquake to cause liquefaction then being evaluated

Table 10. Prediction of liquefaction potential of Gilan plain (northwestern Iran) using a multilayer neural network classification method

Location No.	O_1	O_2	O_3	O_4	O_5	Previous observation (Liquefied/Nonliquefied)
1	0.9476					liquefied
2	0.9476					liquefied
3	0.9269					liquefied
4	0.8830					liquefied
5	0.9079					liquefied
6	0.8884					liquefied
7	0.9476					liquefied
8	0.9672					liquefied
9	0.9783					liquefied
10	0.9079					liquefied
11	0.9476					liquefied
12	0.9476					liquefied
13			0.9920			liquefied
14	0.9920					liquefied
15	0.4206					liquefied
16	0.9795					liquefied
17	0.9553					liquefied
18	0.8150					liquefied
19	0.9920					liquefied
20	0.9932					liquefied
21	0.8800					liquefied
22	0.9532					liquefied
23	0.9913					liquefied
24	0.8815					liquefied
25	0.5892					liquefied
26	0.9918					liquefied
27	0.9432					liquefied
28	0.9614					liquefied
29	0.5402					liquefied
30	0.7966					liquefied
31	0.0434					liquefied
32			0.0345			unknown area
33				0.0308		unknown area
34	0.0737					unknown area
35				0.1337		unknown area
36		0.0738				unknown area
37					0.0507	unknown area
38				0.0328		unknown area
39				0.1439		unknown area
40		0.0890				unknown area
41					0.0507	unknown area
42				0.0583		unknown area
43					0.0155	nonliquefied
44		0.0433				unknown area
45				0.0826		nonliquefied
46			0.1097			liquefied
47			0.0414			unknown area
48		0.427				unknown area
49			0.0126			unknown area
50					0.0335	nonliquefied
51					0.1425	nonliquefied
52			0.4910			unknown area
53	0.0218					unknown area
54				0.1399		nonliquefied
55					0.0141	nonliquefied
56					0.0141	nonliquefied

Locations No. 1 to 30 located in Astaneh area; Locations No. 31 to 42 located in Rasht area; Locations No. 43 to 46 located in Lahijan area; Locations No. 47 to 49 located in Langroud-Amlash area; Locations No. 50 to 53 located in Siyahkal area; Locations No. 54 to 56 located in Sangar area.

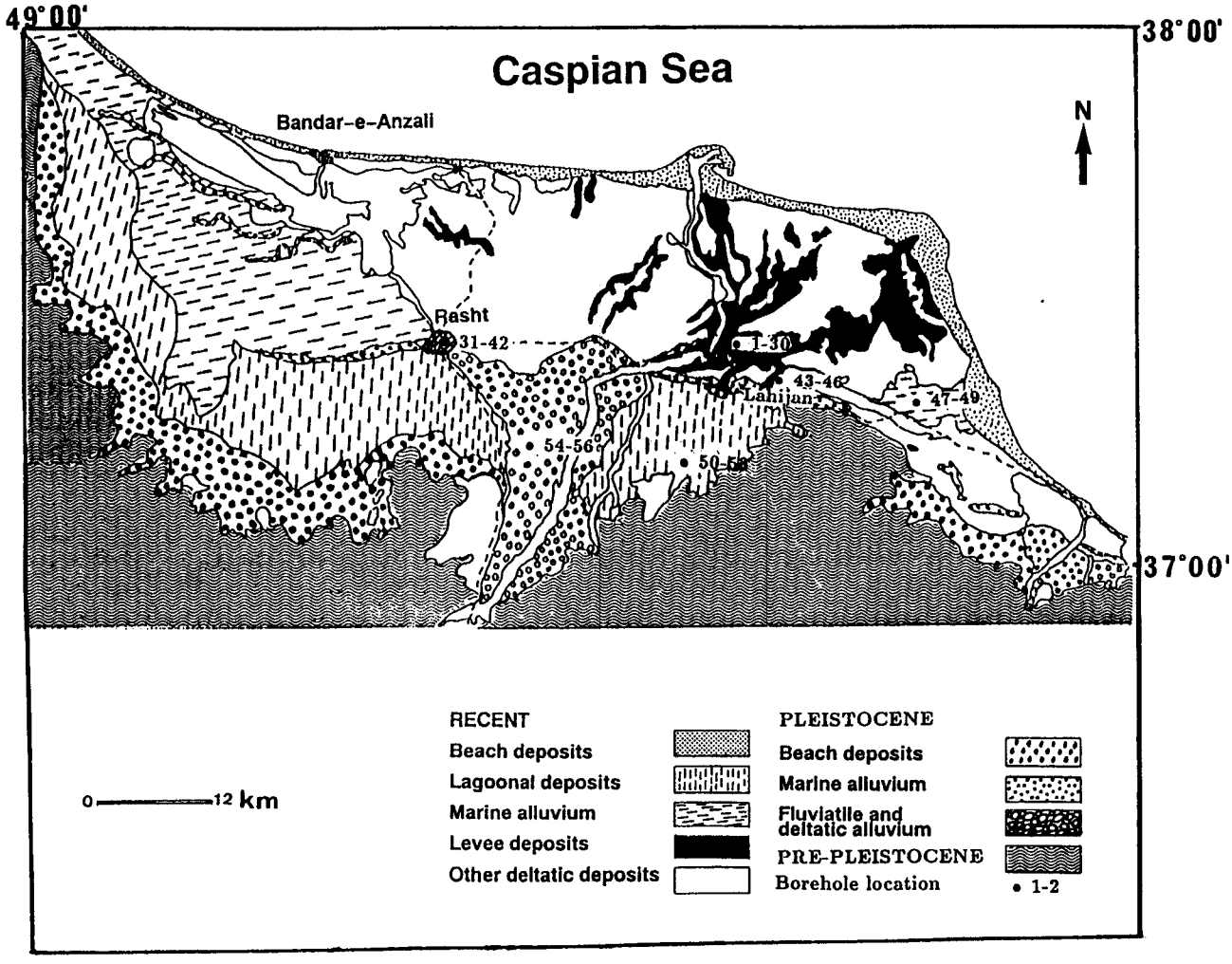

Figure 4. Geological map of Gilan plain (northwestern Iran) [Nogole Sadat, 1992, preprint Geological Map of Gilan]

separately.

We used the prediction ability of the artificial neural network to simultaneously evaluate the susceptibility of soils to liquefaction and the ability of earthquakes to cause liquefaction, which was the goal of this study, by considering the criteria given in Tables 1-5.

We used the application of pattern recognition of neural networks to assess the liquefaction potential, this application has been well known for a much wider range approach. Our neural network approach is fundamentally different from other structures of neural networks. We used the key of pattern recognition of neural networks to predict a hazard rate of liquefaction potential. The proposed neural networks structure corresponds to arbitrary input patterns that give a prediction output according to a desired value which is very fast and highly accurate in predicting phenomena for natural hazard microzoning. The applicability of the method for the prediction of liquefaction potential of soils was examined in the northwest of Iran (Gilan area), and the results of this examination are given in Table 10. Figure 4 illustrates the location of the evaluated points. The locations 1 to 30 are those which showed widespread liquefaction during the 1990 Iran-Manjil earthquake, and their calculated liquefaction potential is very high except for point 13, which calculated as a moderate potential. However, the calculated rate of this point is 0.992 in output class $3(O_3)$ which is very close to class number 2 or the high liquefaction potential class. The calculated liquefaction potential rate for point number 31 is 0.0434 in output class $1(O_1)$, the rate of which is larger than other output rates.

Acknowledgements

The authors wish to extend their deepest appreciation and gratitude to Dr. M.A.A. Nogole Sadat of the

Geological Survey of Iran and Mr. A. Johanbakhash of the Ministry of the Interior of the Islamic Republic of Iran for their helpful guidance and collaboration in providing the necessary facilities during the fieldwork and collection of data and for supplying the topographical and geological maps of Gilan.

References

1. Ohsahi, Y. Niigata earthquakes, 1964 building damage and condition, soil and foundations. *Japanese Soc. of Soil Mechanics and Foundation Engineering*, **6**, (2), 14-37, (1966).
2. Seed, H.B. Landslides during earthquakes due to liquefaction. *J. SMFD, ASCE*, **94:SM5**, 1053-1122, (1968).
3. Ishihara, K. and Perlea, V. Liquefaction associated ground damage during the Varancea earthquake of March 4, 1977. *Soil and Foundation Engineering*, **24**, (1), 90-112, (1984).
4. Iwasaki, T. Soil liquefaction studies in Japan. *Soil Dynamics and Earthquake Engineering*, **5**, (1), (1986).
5. Seed, H.B. *et al.* Principal geotechnical aspects of the 1989 Loma prieta earthquake. *Soil and Foundations*, **31**, (1), 1-26, (1991).
6. Fatemi Aghda, S.M., Suzuki, A., Nogole Sadat, M.A. and Kitazono, Y. Evaluation of geological engineering aspects of quaternary sediments in northwest of Iran. 29th International Geological Congress, Abstracts Vol. 3, pp. 856, Kyoto, Japan, (1992).
7. Seed, H.B. and Idriss, I.M. Simplified procedure for soil liquefaction potential *J. SMFD, ASCE*, **97**, (9), 1249-1273, (1971).
8. Seed, H.B. and Idriss, I.M. Ground motions and soil liquefaction during earthquakes. Monograph series, ISBN 0-943198-24-0. Earthquake engineering research institute, Berkeley, California, (1982).
9. Iwasaki, T., Tatsuoka, F., Tokida, K. and Yasuda, S.A. A practical method for assessing soil liquefaction potential based on case studies at various sites in Japan. *Proc. of 2nd Int. Conf. on Microzonation*, **2**, 885-896, (1978).
10. Youd, T.L. and Hoose, S.N. Liquefaction susceptibility and geologic setting. *Proc. 6th World Conf. on Earthquake Engineering, New Dehli, India*, **6**, 37-42, (1978).
11. Elton, D. and Hadj-Hamou, T. Liquefaction potential map for Charleston, South Carolina. *J. GED, ASCE*, **116**, (2), 244-265, (1990).
12. Youd, T.L. and Perkins, D. Mapping of liquefaction severity index. *Ibid.*, **113**, (11), 1374-1392, (1987).
13. Kavazanjian, E., Roth, R.A. and Echezuria, H. Liquefaction potential mapping for San Francisco. *Ibid.*, **111**, (1), 54-76, (1985).
14. Wakamatsu, K. Evaluation of liquefaction susceptibility based on detailed geomorphological classification. Abstract, Annual Meeting of Architectural Institute of Japan, Vol. B, pp. 1443-1444, (in Japanese), (1992).
15. Medvedev, J. *Engineering Seismology*. Academia Nauk Press, Moscow, (1962).
16. Evernden, J.F. and Thomson, J.M. *Predicting seismic intensities*. U.S. Geological Survey Profes. Paper 1360, U.S.G.S., pp. 151-202, (1985).
17. Kagami, H., Okada, S. and Ohta, Y. Versatile application of dense and precision seismic intensity data by an advanced questionnaire survey. *Proc. Ninth World Conf. on Earthquake Eng.*, **8**, 937-942, (1988).
18. Astroza, M. and Monje, J. Regional seismic zonation in central Chile. *Proc. Fourth Inter. Conf. on Seismic Zonation*, **3**, 487-494, (1991).
19. Borcherdt, R.D. and Gibbs, J.F. Effects of local geological conditions in the San Fransisco bay region on ground motions and the intensities of the 1906 earthquake. *Bull. Seis. Soc. Am.*, **66**, 476-500, (1976).
20. Shima, E. Seismic microzonation map of Tokyo. *Proc. Second Inter. Conf. on Microzonation*, **1**, 433-443, (1978).
21. *Neural networks: Theoretical foundations and analysis*, (ed. C. Lau), pp. 3-24. New York: IEEE Press, C(1992).
22. Sugisaka, M. and Teshnehlab, M. Pattern classification of processed foodstuffs via artificial neural networks. *Reports of the Faculty of Engineering, Oita University*, (24), 7-13, (1991).
23. Sugisaka, M. and Teshnehlab, M. Fast pattern recognition using moment invariants computation via artificial neural networks. *Control Theory and Advanced Technology, C-TAT*, **9**, (4), 877-886, (Dec. 1993).
24. Teshnehlab, M. Dynamic pattern recognition using moment invariants computation via artificial neural networks. MSc Thesis, (March 1992).
25. Shibata, T. *Hierarchical intelligent control of robotic motion*. Ph.D. Thesis, (March 1992).
26. Teshnehlab, M. *Neural network-based controls using flexible neuron models*. Ph.D. Thesis, (March 1995).
27. Teshnehlab, M. and Watanabe, K. Control strategy of robotic manipulator based on flexible neural network structure, *An Industrial decision making and control*, pp. 385-398, Kluwer Academic Publishers, (1994).
28. Teshnehlab, M. and Watanabe, K. Neural network controller with flexible structure based on the feedback-error-learning. *Journal of Intelligent and Robotic Systems*, (submitted 1996).
29. Teshnehlab, M. and Daghighi, A. Control of multivariable processing using flexible neural networks. *Proceedings of ICEE-98, Control Volume*, (1998).
30. Teshnehlab, M. and Afiyuni, D. Intelligent control of highway traffic density using neural network and fuzzy-neural network. *Proceedings of Third Iranian Traffic Engineering Conference*, (Feb. 1998).
31. Berberian, M., Qorashi, M., Jackson, J.A., Priestley, K. and Wallace, T. The Rudbar-Tarom earthquake of 20 June 1990 in NW Persia: Preliminary field and seismological observations and its tectonic significance. *Bul. S.S. of America*, **82**, (4), 1726-1755, (1992).
32. Fatemi Aghda, S.M., Suzuki, A. and Kitazono, Y. *Evaluation of cohesionless soils behavior in northwestern part of Iran (Gilan plain)*, pp. 290-291. 47th Annual Meeting of JSCE, (1992).
33. Fatemi Aghda, S.M., Suzuki, A. and Kitazono, Y. *Evaluation of geotechnical properties of Quaternary*

sediments in northwestern part of Iran (Gilan plain) using multiple regression analysis, pp. 562-563. Annual Meeting of JSCE West Branch (Seibu), Fukuoka, Japan, (1992).

34. Ghayoumian, J., Fatemi Aghda, S.M., Koike, K., Doi, E., Nogole Sadat, M.A. and Nakajima, S. Construction and application of a geotechnical data base for preparation of engineering geological maps for northwestern Iran. *Geoinformatics*, **4**, (3), 273-282, (1993).
35. Nogole Sadat, M.A. Geological Engineering Investigations of Gilan. Unpublished report. Construction Dept. of the Gilan Governmental Office, (1991).

Correction

Regrettably, the following errors occurred during the final layout process of the previous issue (Vol. 9, No. 1, Winter 1998, Zemestan 1376, *J. Sci. I.R. Iran*) beyond the journal management's control. They are hereby corrected:

a) P. 38: In line 3 of the legend for Plate 2, part of the sentence was missed out completely which is shown here:

"(2) PPL view of transformation of pyroxenes to biotite (Bi) due to metasomatic action of granite on norite"

b) P. 46: In the left column, lines 1 and 2 of the first paragraph were misplaced; It should read:

"of 920°C, beyond which none of the minerals are stable.
If H_2O is about 5%, biotite disappears below, 900°C and"